

## REVIEW ARTICLE



## FDG PET/MR Imaging in Major Neurocognitive Disorders

Ismini C. Mainta<sup>1</sup>, Daniela Perani<sup>2</sup>, Bénédicte M.A. Delattre<sup>1</sup>, Frédéric Assal<sup>1,3</sup>, Sven Haller<sup>3</sup>, Maria I. Vargas<sup>1,3</sup>, Dina S. Zekry<sup>1,3</sup>, Giovanni B. Frisoni<sup>1,3</sup>, Habib Zaidi<sup>1,3</sup>, Osman Ratib<sup>1,3</sup> and Valentina Garibotto<sup>1,3,\*</sup>

<sup>1</sup>Geneva University Hospital, Geneva, Switzerland; <sup>2</sup>Vita Salute San Raffaele University and San Raffaele Hospital, Milan, Italy; <sup>3</sup>Geneva University, Geneva, Switzerland

**Abstract:** PET/MRI tomographs represent the latest development in hybrid molecular imaging, opening new perspectives for clinical and research applications and attracting a large interest among the medical community. This new hybrid modality is expected to play a pivotal role in a number of clinical applications and among these the assessment of neurodegenerative disorders. PET and MRI, acquired separately, are already the imaging biomarkers of choice for a comprehensive assessment of the changes occurring in dementias (major cognitive disorders) as well as in their prodromal phase.

In this paper we review the current evidence on the use of integrated PET/MRI scanners to investigate patients with neurodegenerative conditions, and in particular major neurocognitive disorders. The number of studies performed is still limited and shows that the use of PET/MRI gives results overall comparable to PET/CT and MRI acquired independently. We also address the challenges for quantitative aspects in PET/MRI, namely attenuation, partial volume and motion correction and the use of semi-quantitative approaches for FDG PET image analysis in this framework.

The recent development of PET tracers for the *in vivo* differential diagnosis of dementias, able to visualize amyloid and tau deposits, suggests that in the future PET/MRI might represent the investigation of choice for a single session evaluation of morphological, functional and molecular markers.

**Keywords:** PET, fluorodeoxyglucose, MRI, hybrid imaging, statistical parametric mapping, major cognitive disorders.

## 1. INTRODUCTION

Dementias (major neurocognitive disorders according to the Diagnostic and Statistical Manual of Mental Disorders, Vth edition), given their strong association with age, are increasingly prevalent with increased life expectancy and are one of the most relevant causes of disability and dependency among elderly people, with strong social and economic impact [1, 2].

The pathophysiological processes start early before the clinical symptoms are installed [3]. The diagnosis and the differential diagnosis among the different forms is a critical process, especially in the early phases, such as in patients diagnosed with Mild Cognitive Impairment (MCI). In MCI, it is particularly important to identify those individuals deemed to progress to major neurocognitive disorder for proper management and symptomatic treatment [4, 5]. How-

ever, clinical diagnosis even among experienced physicians is inaccurate in about 10-15% of cases, mainly in the early phases. For this reason, the development of diagnostic or prognostic biomarkers to support clinical diagnosis is imperative for this condition that preoccupies families, treating physicians and by extension the whole community [6].

A biological marker or biomarker is defined as a characteristic that is objectively measured and evaluated as an indicator of normal biological processes, pathogenic processes or pharmacologic responses to a therapeutic intervention [7]. Ideally, a biomarker should be able to detect a hallmark-feature of the pathophysiological processes active in different types of dementia, it should be validated in neuropathologically confirmed cases; it should be reliable, minimally invasive and simple to perform [8]. In addition, an ideal biomarker should be able to identify subjects in prodromal phase or at risk, in the preclinical phase, when the pathogenesis of the disease is already ongoing, but before full clinical onset [9, 10].

It seems rather unlikely that one specific biomarker exists. Instead, a combination of biomarkers that will allow the

\*Address correspondence to this author at the Geneva University and University Hospital, Rue Gabrielle Perret Gentil 4, 1205 Geneva, Switzerland; Tel: +41 795534459; Fax: +41 22 3727169; E-mail: valentina.garibotto@hcuge.ch

best support for early diagnosis and differential diagnosis is a more realistic approach. As the access for histopathologic analysis of the brain is not feasible *in vivo*, neuroimaging arises as the closest possibility [11].

## 2. PET AND MR IMAGING AS BIOMARKER OF NEURODEGENERATION

Among imaging modalities, magnetic resonance (MR) and positron emission tomography (PET), complementary one to the other, are the methods of choice for neuroimaging [12].

MRI, the first-line modality for most of neurological indications, provides detailed description of gray and white matter anatomy, brain vasculature, blood brain barrier integrity and other functional parameters. In the diagnostic work-up, MRI structural imaging was traditionally used to rule out potentially reversible brain processes mimicking the clinical symptoms of neurodegenerative diseases such as brain tumors, strokes, chronic subdural hematomas, inflammatory diseases, normal pressure hydrocephalus. It was also used to detect characteristic patterns of regional atrophy, possibly supporting the differential diagnosis of main major neurocognitive disorders [13]. In a recent review, it was found that volumetry of brain atrophy can discriminate healthy elderly subjects from patients who then progressed from MCI to Alzheimer's disease (AD) with limited specificity and sensitivity [14]. Novel promising MR techniques have emerged recently. The resting-state fMRI allows an assessment of changes in brain resting state functional connectivity networks, such as the default mode network. Resting-state fMRI has revealed either compensational increases or disruption of functional interconnectivity, later in the course of the disease, in brain areas susceptible to amyloid deposition in patients with AD [15-17]. Diffusion tensor imaging (DTI) as a tool of structural interconnectivity of the brain, can identify subcortical fiber tract disruptions and can be used to point out to different types of dementia disorders [17-19]. These results however were obtained at a group level, and further validation and standardization at single subject level is mandatory.

Notably, arterial spin labeling (ASL) a sophisticated technique of MR perfusion, was shown to provide patterns of decreased blood flow in patients with AD that resemble the typical diagnostic patterns of FDG PET hypometabolism [17, 20-22].

In addition, in the case of vascular dementia, MRI offers an exact cartography of cortical and subcortical infarcts. Traditionally this type of dementia was regarded as a clearly separate entity from neurodegenerative dementia. However, recently it is considered that there is a spectrum between pure vascular and pure neurodegenerative dementia, with special reference to AD, where in a large majority both neurodegenerative and vascular causes contribute to the clinical expression of dementia [23, 24], and assessment of morphological and functional imaging proves necessary in cases which in the past would have been directly classified as cerebrovascular dementia without further work-up.

On the other hand, PET with a continuously increasing panel of available radiotracers offers quantitative *in vivo*

functional investigation of the brain [25]. Among these, two play a major role in the diagnosis of AD, namely FDG and amyloid imaging markers. This is already implemented in the new diagnostic criteria for AD and MCI [26-28].

FDG is a sensitive and specific method for early identification of AD pathology, for differential diagnosis from other types of dementia as well as for prediction of AD, even in the mild and asymptomatic stages [3, 29-31]. Cerebral glucose metabolism primarily reflects synaptic activity and neuronal integrity, long before morphological changes are installed [17]. Different specific patterns of regional glucose metabolism indicating neuronal dysfunction have been identified in each form of dementia. In AD, the characteristic FDG pattern is a decrease of the metabolic activity in the precuneus/posterior cingulate and bilateral parietotemporal cortex with 93% sensitivity and 76% specificity [32] or up to 96% and 84% respectively using voxel-based methods [33]. An example of this typical pattern of hypometabolism, in comparison with the pattern typically observed in cases of dementia with Lewy bodies (DLB), which is characterized instead by a preserved metabolism in the posterior cingulate gyrus and a reduced occipital metabolism, is shown in Fig. (1). There is evidence that the medial temporal lobes, and in particular the hippocampus, are also severely affected in AD. In a multicenter study, the combination of the cortical deficits and hippocampal hypoactivity was shown to increase specificity from 71% to 100% in differentiating AD from DLB and from 65% to 94 % in differentiating AD from FTD. In the same study, FDG could be used to discriminate MCI from normal subjects with 86% sensitivity and 96% specificity [34]. In a prospective study, FDG PET was proven to be a valuable diagnostic tool for the prediction of clinical progression of MCI patients to AD, or other dementia conditions with very high sensitivity and specificity [30, 35, 36]. In a retrospective study of MCI patients, PET FDG was found to increase physician's confidence in the diagnosis of AD lowering the number of unclear diagnoses from 39.4% to 16% of cases [37]. FDG uptake, as a functional test, is non-specifically reduced also in the presence of vascular lesions, and for this reason the integration of PET and MRI information is of utmost importance, as exemplified in Fig. (2).

Recently, new PET tracers were made available for *in vivo* non-invasive detection of  $\beta$ -amyloid plaques, a key pathological signature of AD. Cortical amyloid accumulation can be detected years, even decades, before the onset of cognitive decline and it has been reported as the earliest biomarker to show a measurable abnormality [38]. It is assumed to represent an early event in AD, leading ultimately to cognitive decline, even if the interplay between amyloid and neurodegenerative phenomena is still largely unknown and the "amyloid cascade hypothesis" has been questioned by recent evidence [17, 39]. This debate does not limit the relevance of amyloid imaging as an accurate marker of amyloidosis and the first molecular marker for the differential diagnosis of dementias *in vivo* [40]. A negative amyloid PET excludes AD as the underlying pathology, with high negative predictive value (100% using C-PIB) and specificity (91% using florbetaben) [17, 41, 42]. It may help to discriminate MCI subjects that are likely to progress to AD over the next

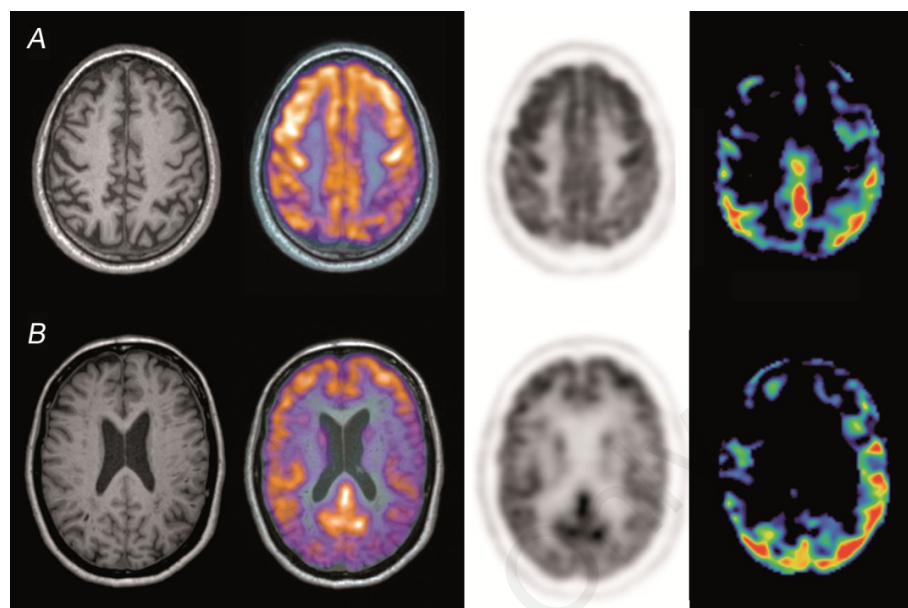


**Fig. (1).** The figure shows MRI, fused PET/MRI, FDG PET distribution images and parametric images of deviation from the normal database (BRASS software) of two cases evaluated for cognitive impairment, with two different hypometabolic pattern: in the first row the reduction in the posterior cingulate cortex, precuneus and lateral parietal cortex is typical for AD, while in the second row the preservation of posterior cingulate metabolism is a feature for DLB.

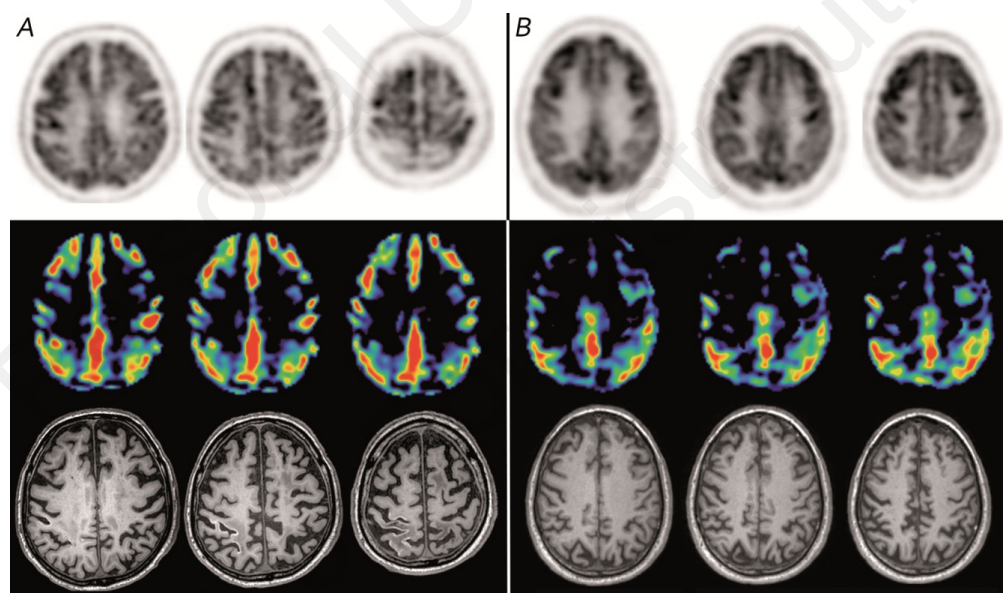


**Fig. (2).** The figure shows two cases evaluated for cognitive impairment, with a similar metabolic pattern of hypoactivity in posterior cortical regions, of different etiology, as proven by MRI: case A has vascular lesions, while case B has a normal MRI.  
First row: FDG PET distribution images.  
Second row: parametric images of deviation from the normal database (BRASS software).  
Third row: T1w MR images.

3-5 years, with less than 10% of amyloid PET negative MCI patients finally developing AD [43]. Furthermore, dynamic acquisition immediately after iv injection has been proposed to highlight areas of reduced cerebral perfusion.

Preliminary results showed that the initial 5 minutes frame from 1 to 6 minutes post injection of amyloid-tracer is potentially useful in providing FDG-like information [44, 45]. However, 20-30% of normal elderly individuals have a

detectable amyloid deposition [46]. The prevalence of cerebral amyloid increases from 10% - 15% at age 65 y.o. to about 50% at age 85 y.o. [38]. Moreover, amyloid PET is positive in cerebral amyloid angiopathy [47] and in 50-70% of cases of another common major neurocognitive disorder that is dementia with Lewy bodies [48]. In conclusion, amyloid PET cannot establish the diagnosis of AD, but it should

be considered more as an additional biomarker when the clinical context is in favor [47].

For a long time, parallel analysis of information obtained separately with each modality served the medical and research community.

Recently, new hybrid technologies capable of acquiring both PET and MRI images in a single session became available (1. Ingenuity TF PET/MR system of Philips, a sequential system, 2. Biograph mMR of Siemens, a simultaneous PET/MR system and 3. SIGNA PET/MR of GE, a simultaneous system). In this review, we discuss the recent advances of hybrid PET/MR in major cognitive disorders with special focus on Alzheimer's disease, as well as the challenges of this hybrid modality.

### 3. PET/MR TECHNOLOGY

Most PET systems currently in use combine PET and Computed Tomography (CT) in the form of PET/CT hybrid systems.

The added value of PET/CT vs. PET alone has been consistently shown, mainly for oncological applications, while for neurological application the contribution of non-contrast enhanced low dose CT of brain imaging is limited.

A decade after the introduction of PET/CT, the advent of hybrid PET/MR tomographs, capable of acquiring both modalities into one imaging session, has been thus considered a major outbreak for neurological imaging.

This technology has been first tested in humans in 2008 [49] and only in 2010 the first commercial systems have been deployed.

A number of contributions describe in details the characteristics of the various solutions available and major challenges had to be overcome in order to bring these two modalities together [49-54], we will only briefly summarize here the main distinctive features.

First, PET and MR images can be acquired sequentially or simultaneously. The sequential setup, analogous to the structure of the PET/CT tomographs, has two separate scanners connected by a bed, which avoids repositioning of the patients and offers the opportunity to acquire the two sets of images in one single imaging session [55, 56]. In this design smaller modifications to each modality (type of coils for the MR, detector technology for the PET) are required, and both PET and MRI can be considered equivalent to standalone systems. Clearly, a sequential setup results in a longer acquisition time, which is the sum of the acquisition time necessary for PET and MRI evaluation. An example of a typical protocol designed for the assessment of neurodegenerative dementia on a sequential system is provided in Fig. (3).

The simultaneous acquisition is preferable to fully exploit the combination of the two modalities, thus reducing the total examination time and enabling continuous recording of MR images during PET acquisition for motion correction, for example, as described in section 3. However, for the combination of both modalities in a single gantry, specific requirements for both PET and MR subsystems have to be met to avoid potential interference between the two scanners.

For this reason, MR-compatible detectors had to be developed to enable the implementation of such systems. This includes avalanche photodiode (APD) and Silicon photomultiplier (SiPM) readout technologies which are actually used on commercial PET-MR systems. However, the time-of-flight (TOF) technology, considered to be an important asset to improve PET image quality and enhance signal-to-noise ratio, is not provided by one of the two simultaneous systems commercially available today owing to the low timing resolution of APDs [57, 58]. In addition, in simultaneous acquisition, concerns about the effect of the magnetic field on the positrons travel range in high-energy radioisotopes has been raised [59].

Aside from commercially available systems, research tomographs developed in academic settings are also being exploited for studies combining the two modalities. One such example, a shuttle system connecting a 7T MRI to a high resolution brain dedicated PET scanner has been recently used for investigating smaller brain structures, such as the hippocampus, with promising results [60, 61].

### 4. TECHNICAL CHALLENGES FOR PET/MR IN DEMENTIA

#### 4.1. Attenuation Correction

Attenuation correction is a prerequisite in quantitative PET imaging. The two annihilation 511keV photons traversing the human body are subjects to interactions with biological tissues, the main being Compton scattering. In contrast to SPECT imaging, two annihilation photons have to be detected for the event to be registered and the attenuation depends on the total intra-body distance travelled by both annihilation photons [62]. As such, to enable quantitative and qualitative assessment of the radiotracer's regional uptake, a measurement of photon attenuation should be performed to correct and redistribute the activity backwards. Until recently, transmission scans have been used for this purpose, using either positron- or gamma-emitting transmission sources or x-ray tubes, enabling to build patient-specific attenuation maps reflecting the electronic density. However, this information is not easily extracted, from MRI where the intensity depends on proton density and relaxation times [63-65].

MR-based attenuation correction was first developed for brain PET imaging, using three main approaches: segmentation-based approaches, atlas registration and machine learning techniques and emission-based approaches.

In the template-based approach, an average attenuation map template is generated by a number of available  $^{68}\text{Ge}$  transmission scans spatially normalized to the standard brain of SPM. With non-linear registration of the T1 weighted MRI co-registered template of SPM to the MRI of the patient, a warping matrix is obtained. This warping matrix is applied to the average attenuation map template to obtain an attenuation map adapted to the patient [63, 66, 67].

In the atlas-based approaches, a database of MR and co-registered CT brain images is employed integrating global anatomical knowledge. Non-rigid registration methods are commonly applied, where all MR atlas data sets are warped to the patient's MR image, and the same transformations are

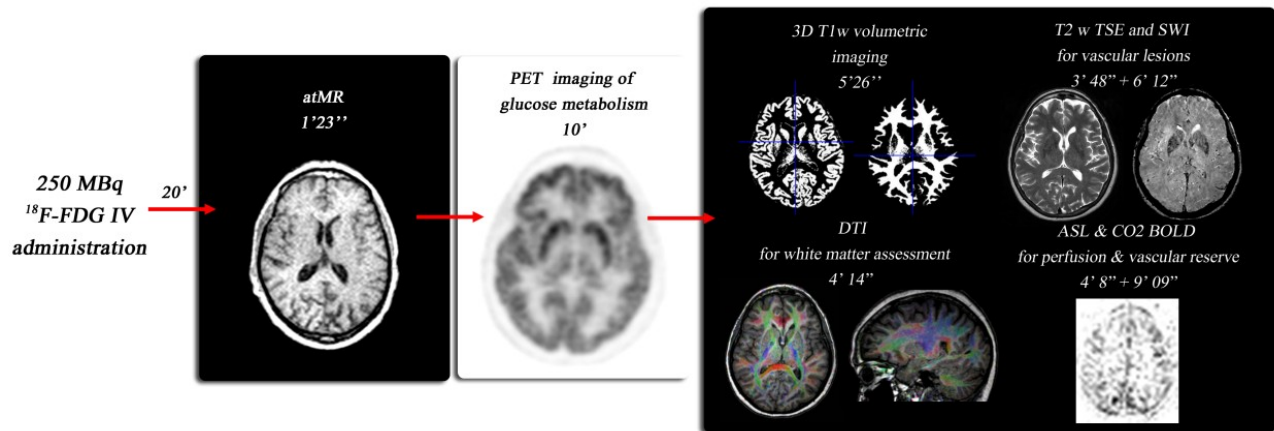


**Fig. (3).** Example of a protocol designed for a comprehensive evaluation of functional and anatomical abnormalities in neurodegenerative dementia in a sequential PET/MRI system: the whole evaluation lasts about 50 minutes.

then applied to the CT atlas data sets enabling to obtain a patient-specific pseudo-CT. Thereafter, similar to PET/CT scanners, the CT Hounsfield units are scaled to PET attenuation coefficients to derive the attenuation map which is finally forward projected to generate attenuation correction factors for the correction of the emission scan. Alternatively, the MR atlas database can be co-registered to a labeled image of segmentation into different tissue classes, which after warping to the patient's MR image generates the corresponding attenuation map [63, 64, 66, 68, 69]. More sophisticated approaches for brain imaging involving the use of multi-atlas information propagation schemes were also recently reported [70].

In the segmentation based approach, T1 weighted MR image is directly segmented and classified into different tissue types. Tissue-specific attenuation coefficients at 511keV are assigned, defining the attenuation map. The current commercially available systems have implemented a routine segmentation of dedicated MR images into air, lung and soft tissue [71] or air, lung, fat and soft tissue [72]. The attenuation correction map measured for the scanner table and head coils is then summed to the attenuation estimated from body segmentation, as exemplified in Fig. (4). Neither segmentation method takes into account bone attenuation [73].

In conventional MR Dixon sequences, bone and air filled cavities (ethmoidal cells, sphenoidal sinus, mastoid processes, frontal and maxillary sinuses) are almost assigned the same intensity range, while the densities of these tissue types are completely different, affecting the reconstructed PET images in brain structures in proximity [74]. A recent study reported that ignoring bone during attenuation correction introduces strong spatially varying bias of the PET activity in PET/MR images [73]. In another study, comparing the performance of PET/CT and PET/MR, region-dependent differences were also found that could partially be explained by differences in the attenuation correction algorithm, while they found deviations even in the non-attenuation corrected images, justifying further investigation [11]. Sophisticated segmentation methods have been proposed over time in order to include bone attenuation, but are not yet integrated into clinically available software [68, 75-77].

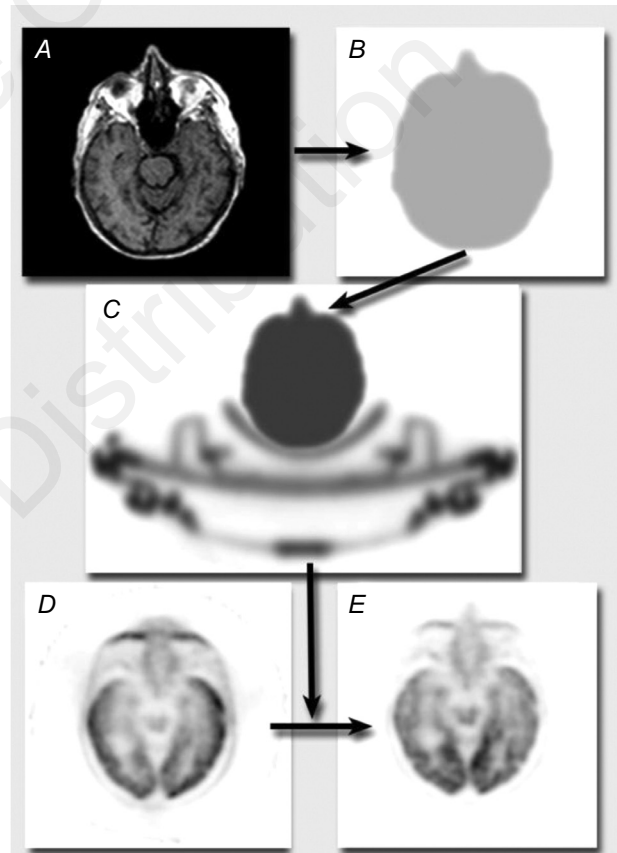


**Fig. (4).** Schematic representation of the attenuation correction process adopted for brain PET scans on the Philips Ingenuity TF PET/MRI: the homogeneous attenuation (B) estimated from segmenting MRI (A) is added to the measured attenuation map calculated of head coils and scanner table (C). Both uncorrected (D) and corrected (E) PET are shown.

With dedicated MR sequences (ultrashort echo time UTE, DUTE, Zero time eco ZTE), bone tissue can be differentiated from air. The combination of UTE (for bone-air separation) and Dixon (for soft tissue-fat separation) enables to obtain a four tissue-class attenuation map. However, se-

quential application of these sequences is time-consuming and makes the protocol complex, especially in case of patient motion. Alternatively, with a new triple-echo UTE (UTILE) MR sequence, distinction of four tissue classes (bone, air, soft and adipose tissue) is achievable with post-processing procedures, obtaining all information required for an accurate attenuation estimation with MR images [78, 79].

In the attenuation correction procedure, we must also take into account the attenuation caused from radiofrequency coils, the examination table and other possible devices of high-density materials. Attenuation must be measured and added to the attenuation map at the exact location. Templates of coils' attenuation could be generated from CT scans or preferably from PET transmission scans, as conversion from CT to PET energy is not validated for non biological materials and they are more accurate and artifact free compared to CT based templates [63].

More recently, new and promising approaches for estimation of the attenuation correction map based on the emission scan and exploiting the TOF PET information have been developed and are increasingly being characterized [80-82]. When validated in larger series they might represent the ideal and most efficient solution for the attenuation issue in PET/MR systems equipped with TOF technology.

#### 4.2. Motion Correction

In the last decades, the resolution of PET scanners has improved up to approximately 2-3mm full width half maximum (FWHM) in brain studies [83]. But as the resolution increases, image blurring due to patient's motion becomes more evident, reducing the effective spatial resolution as low as 1cm [84]. Head restraints are commonly applied to eliminate motion of large amplitude, but image degradation due to small movements persists [85, 86]. Methods for correction of inherent movements have been developed. A simple technique is the inter-frame correction, where the head is monitored with a motion-tracking system and each time a movement above a certain threshold is detected, PET data are registered into a new frame [87]. More accurate rigid motion correction can be achieved with event-based correction techniques, where PET data are acquired in a list-mode format with simultaneous monitoring of the patient's motion with a motion-tracking system. Simultaneous hybrid PET/MR acquisitions have the advantage that motion tracking can be based on the acquired MR data, offering high-temporal-resolution motion estimates [88]. Motion detected on the MR images is used to transform both emission and attenuation correction data, eliminating blurring without reducing the signal to noise ratio [89]. Recent phantom and *in vivo* studies have proved that MR-based motion correction can improve PET image quality, quantitative accuracy and increase reliability and reproducibility of PET data, which is of particular interest in patients with limited compliance, such as in dementing disorders [29, 88, 90]. Furthermore, a recent study involving patients and healthy volunteers, has demonstrated that motion registration could even be used for diagnostic purposes, as the accumulated global head rotation itself significantly discriminated controls from MCI and AD patients [91].

#### 4.3. Partial Volume Effect Correction

In order to improve PET quantification accuracy, one must not forget the Partial Volume Effect (PVE). Compensation for PVE is mandatory in order to distinguish the loss of radiotracer uptake due to PVE from the true metabolic decline [92]. The activity signal from structures smaller than 2-4 times the full width at half maximum of the scanner's point spread function is subject to the PVE. As the thickness of the cortical gray matter is comparable to the spatial resolution of current PET scanners, the brain PET signal is affected by the PVE. This underestimation is accentuated in cases of brain atrophy, which is a hallmark of dementia disorders [29, 92, 93]. MRI with high soft-tissue contrast can be used to estimate the morphological framework from which the PET signal is emitted [93]. Several methods for PVE correction have been proposed, including region-based, voxel-based, with or without additional information for MRI and statistical iterative reconstruction techniques incorporating PVE correction during the reconstruction process [29]. The accuracy of PVE correction methods is affected by factors such as segmentation and spatial coregistration of MRI and PET images, characterization of the scanner's point-spread function, and the assumptions made during the correction [29, 92]. In the case of simultaneous PET/MR acquisitions spatial coregistration is eliminated as a problem. However, in the context of dementia, a strict distinction between hypometabolism and atrophy may not be absolutely necessary as both are associated with dementia. PVE may in fact increase sensitivity in discriminating normal from pathological brains [94].

#### 5. FDG PET/MR AND THE USE OF STANDARDIZED ANALYSES

The analysis of FDG PET brain images in dementia is based on the identification of patterns of hypometabolism, which are disease-specific. The visual analysis of the images is a necessary pre-requisite not only for the diagnosis, but also for the identification of possible artifacts, but suffers from subjectivity, very low accuracy [33] and does not allow the definition of a threshold for abnormality. Recent advances in computer-assisted voxelwise statistical analysis of images allowed the development of a number of tools assisting image interpretation and providing more precise and objective measures. All approaches are based on preliminary transformations of the individual image. The patient's scan has to be anatomically standardized to fit a standard stereotactic coordinate system, such as the stereotactic coordinate system proposed by Talairach and Tournoux or the MNI (Montreal Neurological Institute) coordinate system, to compensate for individual variability in size and shape [94, 95]. Several software for spatial normalization to a standard coordinate system have been developed, some of them widely available for research and clinical use [94]. We summarize here only the main features of the packages mostly commonly used for FDG analysis in dementia.

The Human Brain Atlas (HBA; Department of Neuroscience, Karolinska Institute, Stockholm, Sweden) [96] uses MR images to spatially normalize the PET images into a standard coordinate system. The accuracy is limited by the precision that can be achieved by the co-registration procedure to realign the PET and MRI images. In clinical practice

MR images are not always readily available on-line for routine cases: this limitation is clearly overcome in integrated PET/MRI systems [94].

Statistical parametric mapping (SPM; Wellcome Trust of Neuroimaging, London, UK) [97] is among the state-of-the-art packages for voxelwise statistical analysis of neuroimaging including PET, SPECT and MRI modalities. It is well documented, freely available and technically supported by well-established brain imaging centers. Originally, it was developed as a research tool for PET activation studies on healthy volunteers to distinguish which brain structures are significantly activated by a neuroactivation task and it was not intended for clinical use [92]. At a single-subject level, SPM provides the means for generating objective statistical maps through a voxel to voxel comparison with a number of control scans. First, a spatial normalization of brain images into a standard stereotactic space (MNI) has to be performed by an image-warping algorithm of non-linear registration of PET images with a reference PET template. Recently, a new FDG PET template for normalization procedure particularly devoted to the dementia studies has been developed and validated [98]. It is implemented in SPM list procedures and it is freely available.

Then, a Gaussian smoothing has to be applied to correct for interindividual differences and allow the application of the general linear model approach for the subsequent statistical analysis. Parametrical statistical models are summed at each voxel. This results in a statistical parametric map, an image whose voxels values are statistics, producing t-statistical maps of significant changes in distribution [33, 99].

NEUROSTAT (Department of Internal Medicine, University of Michigan, Ann Arbor, MI, USA) [100] was specially designed for statistical comparison between a normal database and diseased brains. It is a software library for image analysis that includes programs for brain activation studies, group comparison, 3-dimensional stereotactic surface projections (3D-SSP) and co-registration of SPECT, PET and MRI. The 3D-SSP technique projects the cortical activity visualized in a 3D volume image onto the brain surface, generating a surface representation of the cortical activity distribution. The spatially normalized individual image set is compared with the standard atlas template, and z-scores are calculated voxel by voxel to identify statistical deviations from the control database. Three-dimensional stereotactic surface projections of z-scores are then generated allowing visualization of FDG uptake abnormalities and evaluation of their extent and precise topography in terms of stereotactic coordinates [34, 92, 94, 95, 99].

Among the commercial software packages, Brain Registration and Automated SPECT Semiquantification (BRASS; Nuclear Diagnostics, Hägerstedt, Sweden) is specifically oriented toward routine clinical SPECT and PET applications. This software matches with automated masking patient images to 3D reference templates created from images of healthy volunteers. It allows two complementary quantitative comparisons, a voxelwise method and an operator-independent predefined VOI analysis covering the whole brain. The first allows a voxel by voxel comparison of individual studies with a mean-and-SD image from a control

group, by means of statistical intensities differences, based on region growing of maximally deviating voxels. An example of this output is shown in Fig. (1). While this technique can localize and quantify small defects, it is sensitive to small registration errors and to the quality of the template. The second technique determines the mean and z scores within the predefined volumes-of-interest. With BRASS, multiple tracer-specific databases are available. A possible drawback is the inhomogeneity of the implemented cameras and the acquisition protocols, which can be corrected by phantom studies and homogenization of protocols [92, 99, 101].

The PMOD software (PMOD Technologies, Zurich, Switzerland) is another commercial multimodality medical imaging package. The PMOD Alzheimer's discrimination analysis tool (PALZ) is a fully automated method for the discrimination between Alzheimer's Dementia and healthy controls, based on a large FDG database of normal subjects acquired in a multicenter trial [102]. After age correction of the FDG uptake, the individual FDG scan is compared voxel by voxel to the reference database, resulting in the PALZ score, which is a sum of the t-values in a predefined AD specific mask. Based on the data of the control group, a 95% prediction limit and error probabilities can be calculated. If the score of brain areas within the mask is outside the 95 % prediction limit, it is considered abnormal and error probability is stated [92, 102, 103].

A special mention has to be made on the role of standard templates used for spatial normalization. Even subtle errors in spatial normalization introduce loss of accuracy with impact on the diagnosis, both in early stages, where changes are subtle and in advanced cases, with severe atrophy. In most FDG PET studies, the standard SPM H<sub>2</sub>O PET template is used for spatial normalization. As in SPM, contrary to NEUROSTAT pure anatomic standardization, the mathematical nonlinear function in anatomical standardization depends not only on the shape but also on the count distribution of the used template, the matching between the individual image and the template is indeed relevant [98]. Appropriate templates, age matched, disease and tracer specific would be ideal. Recently, an FDG PET dementia-specific template was created for SPM spatial normalization, revealing an overall diagnostic accuracy of 94 % (91 % sensitivity and 95 % specificity) [98].

In a study comparing SPM and NEUROSTAT in normal subjects, small differences in standardization were found, no more than 0.21-1.15mm, validating both [104]. In another validation study that included healthy and atrophied brains, SPM and NEUROSTAT yielded similar patterns of metabolic decrease, although the extent of reduction was greater with SPM, which was more affected by the presence of atrophy [94]. In a retrospective study of 88 patients and 112 cognitively normal controls, it was found that SPM voxelwise analysis of PET-FDG improved diagnostic accuracy in dementia and pre-dementia conditions with a sensitivity of 96% and a specificity of 84% compared to 78% and 50% respectively for visual assessment of FDG scans and 91% and 40 % respectively for clinical assessment [33]. Furthermore, SPM maps strongly enhanced confidence in identifying distinct patterns of hypometabolism in MCI patients,

predicting further progression into different dementias, while all subjects that didn't progress were SPM negative [33]. In another study of MCI patients, single-subject SPM analysis of FDG scans was found to have high predictive prognostic value, by identifying either normal brain metabolism or distinct patterns of hypometabolism, allowing recognition of early AD or other types of cognitive decline [30]. In a study of 22 patients and 18 normal controls, the PALZ tool was found to have 100% sensitivity and 83 % specificity, for the diagnosis of AD. This relatively decreased specificity was attributed to an attenuation correction artifact encountered in this study because of the use post-injection transmission scans [105].

The main limitation for the use of automated analyses in PET/MRI is that, given the novelty of this modality, no PET/MRI normal reference database is available yet and the feasibility of using references databases derived from PET/CT has to be properly validated.

## 6. PET/MR STUDIES IN DEMENTIA

Only a few studies have tested so far the use and the impact of PET/MR in major neurocognitive disorders in a clinical setting: the data currently available are summarized in Table 1.

The first studies only reported the feasibility of PET/MR in various brain applications, including degenerative disorders [106, 107].

More recent studies tested prospectively the performance of PET/MR vs the current reference standard, i.e. PET/CT, with discordant conclusions [11, 108].

The first study evaluated 30 patients with clinically suspected AD: PET/MR images consistently underestimated cortical metabolism and overestimated subcortical signal, with some impact on diagnostic decision supported by semiquantitative analysis [11]. This impact was however limited for experienced readers and its clinical relevance is difficult to establish, given that authors did not discuss if the disagreement changed the diagnostic conclusion. However, these results underline the importance of a validated/matched control group for the diagnostic use of FDG PET/MR in dementia.

The second study partially confirms these findings in a smaller mixed group of patients, including three dementia cases, observing a systematic underestimation of SUV values in PET/MR images [108]. Part of the systematic differences observed in this case might be explained by the fact that PET/CT images were acquired at later time points. Despite the differences in absolute values, the correlation between the regional values obtained in the two sets of images was excellent. Unfortunately this study did not investigate regional relative changes and their impact on the diagnostic interpretation.

Finally, one recent study investigated the presence of hypometabolism and atrophy in a simultaneous PET/MRI study in dementia cases [109]. The authors showed a marked variability in the association of atrophy and hypometabolism in different brain regions and in different dementia syndromes, among AD and FTD syndromic variants, that was lower for

primary progressive aphasia and higher for AD and posterior cortical atrophy and with higher sensitivity of semi-quantitative methods as compared with visual reading.

## 7. FUTURE PERSPECTIVES

The main advantage of the hybrid PET/MR technology is the availability of a large panel of structural, functional and molecular biomarkers in one single imaging session. Previous papers have discussed potential improvements that can be specifically obtained using the integrated design, namely improving quantification of tracer uptake by deriving perfusion information from the MR images, or systematically applying partial volume and motion correction, but no studies have yet validated these approaches in patient series [110, 111].

Indeed, all PET/MRI studies performed so far have combined the two acquisitions, using standard protocols for each, without investigating in depth the added value of their integration. A key issue, to be targeted in future PET/MRI studies, will be the identification of which information is really complementary, using the two techniques, and which data are instead redundant, if any.

First, this technology is the ideal tool to develop validation studies comparing MRI sequences to the gold standard PET based perfusion studies, or identifying to which extent fMRI measures can approximate the FDG PET information. Preliminary studies with this design have been performed in healthy controls and in animal models, identifying systematic biases in MRI measures and highlighting the relevance of appropriate validation schemes before a larger use of MRI-derived perfusion estimates [112-114]. This might be of special interest for the validation of other advanced MRI sequences, such as diffusion weighted imaging (DWI), DTI and magnetic resonance spectroscopy (MRS). DWI is already a validated diagnostic tool for the differential diagnosis of dementia syndromes, being able to identify with a high sensitivity and specificity characteristic changes (high signal on DWI and low signal on apparent diffusion coefficient - ADC - maps) in Creutzfeld Jacob disease [115]. ADC images might also show an increased signal associated with the enlargement of extracellular space and neuronal loss, and this has been previously suggested observing increased ADC in MCI in hippocampal regions [116, 117]. The role of MRS is less established, but increasingly investigated in dementia, as recently reviewed [118].

Second, the unique feature of PET imaging, namely the ability to identify nanomolar targets, might be best exploited using molecular tracers, rather than functional tracers such as FDG. In the field of major cognitive disorders significant progress has been made over the last decade, and beyond amyloid imaging, tau tracers have been recently developed and are currently in phase II trials in patients, raising high expectations for an *in vivo* molecular classification of dementias [119]. For tau tracers the systematic availability of brain volumetry, as in integrated PET/MR systems, might represent a significant progress, given that tau deposition primarily occurs in mesial temporal structures, strongly affected by partial volume in PET.

**Table 1.** FDG PET/MR studies in dementias.

References	N. subjects	PET/MR tomograph design	Study design	Main result
[106]	4 (2 FTD, 1 AD, 1 LBD)	Sequential	Feasibility	Full diagnostic quality of both modalities within acceptable acquisition time
[107]	4 (2 AD, 2 progressive supranuclear palsy)	Simultaneous	Feasibility and comparison with PET/CT	High concordance with PET/CT derived semi-quantitative indices
[11]	30 patients with clinically suspected AD	Simultaneous	Comparison with PET/CT	Regional differences between the two sets, with potential impact on clinical assessment
[108]	3 suspected dementia patients	Simultaneous	Comparison with PET/CT	Excellent agreement and correlation between the two sets despite systematic underestimation of SUV values by PET/MR
[109]	24 subjects (FTD and syndromic AD variants)	Simultaneous	Use of standardized analyses for FDG PET data(SPM) and comparison of hypometabolic and atrophy patterns	High variability in the concordance between atrophy and hypometabolism in different regions and syndromes, lower for primary progressive aphasia and higher for AD and posterior cortical atrophy. Higher sensitivity of quantitative methods as compared with visual reading.

Last, the newly developed digital PET technology might be of interest for designing PET inserts MR-compatible for simultaneous PET/MR brain imaging. This technology, currently in use in recent whole body PET/MR and in one PET/CT system, uses solid state detectors, the digital SiPM, in which each APD has its own readout circuit with an integrated Analog to Digital converter (ADC), permitting a direct digital photon count, contrary to conventional analog SiPM. Preliminary studies have tested its applicability in a preclinical scanner [120]. The use of a brain-dedicated PET insert that can be added to any existing MR scanner without any change to the MRI hardware might offer a more flexible solution at lower cost than fully integrated systems [121].

## CONCLUSION

Hybrid PET/MRI opens new perspectives in functional multi-parametric neuroimaging, allowing acquisition of all relevant information in a single session and increasing patient comfort. Combined information from these two cornerstones of neuroimaging, complementary one to the other, compensating mutually for the limits of each modality, can advance our understanding of brain physiology and pathophysiology, yielding high diagnostic value in the dementia work-up with differential diagnosis between neurodegenerative versus cerebrovascular dementia conditions and among the different types, early in the course of the disease. Technical issues, particularly concerning the MR-based attenuation correction have been identified, but with dedicated MR-sequences even this challenge is surmountable. Various sophisticated programs of automated image analysis are available, guarantying objectivity and reproducibility of the diag-

nosis. Hybrid PET/MRI offers the ideal framework for *in vivo* identification of diagnostic hallmarks of dementing disorders and is likely to become the modality of choice for the assessment of brain function.

## CONFLICT OF INTEREST

The authors confirm that this article content has no conflict of interest.

## ACKNOWLEDGEMENTS

Supported by Aetas, Swiss Foundation of Ageing Research, Genève, Switzerland.

## REFERENCES

- [1] Prince M, Bryce R, Albanese E, Wimo A, Ribeiro W, Ferri CP. The global prevalence of dementia: a systematic review and metaanalysis. *Alzheimers Dement* 9(1): 63-75 e2 (2013).
- [2] Dementia, Fact sheet No. 362, USA: WHO (2012).
- [3] Mosconi L, Murray J, Tsui WH, Li Y, Spector N, Goldowsky A, *et al.* Brain imaging of cognitively normal individuals with 2 parents affected by late-onset AD. *Neurology* 82(9): 752-60 (2014).
- [4] Wallin AK, Andreasen N, Eriksson S, Batsman S, Nasman B, Ekdale A, *et al.* Donepezil in Alzheimer's disease: what to expect after 3 years of treatment in a routine clinical setting. *Dement Geriatr Cogn Disord* 23(3): 150-60 (2007).
- [5] Winblad B, Wimo A, Engedal K, Soininen H, Verhey F, Waldemar G, *et al.* 3-year study of donepezil therapy in Alzheimer's disease: effects of early and continuous therapy. *Dement Geriatr Cogn Disord* 21(5-6): 353-63 (2006).
- [6] Zamrini E, De Santi S, Tolar M. Imaging is superior to cognitive testing for early diagnosis of Alzheimer's disease. *Neurobiol Aging* 25(5): 685-91 (2004).

- [7] Atkinson AJ, Colburn WA, DeGruttola VG, DeMets DL, Downing GJ, Hoth DF, et al. Biomarkers and surrogate endpoints: preferred definitions and conceptual framework. *Clin Pharmacol Ther* 69(3): 89-95 (2001).
- [8] Nordberg A. Molecular imaging in Alzheimer's disease: new perspectives on biomarkers for early diagnosis and drug development. *Alzheimers Res Ther* 3(6): 34 (2011).
- [9] Mosconi L. Glucose metabolism in normal aging and Alzheimer's disease: methodological and physiological considerations for PET studies. *Clin Transl Imag* 1(4): 217-233 (2013).
- [10] Perani D. FDG PET and cognitive symptoms of dementia. *Clin Transl Imag* 1(4): 247-260 (2013).
- [11] Hitz S, Habekost C, Furst S, Delso G, Forste S, Ziegler S, et al. Systematic comparison of the performance of integrated whole-body PET/MR imaging to conventional PET CT for 18F-FDG brain imaging in patients examined for suspected dementia. *J Nucl Med* 55(6): 923-931 (2014).
- [12] Haller S, Garibotti V, Kovari E, Bouras C, Xekardaki A, Rodriguez C, et al. Neuroimaging of dementia in 2013: what radiologists need to know. *Eur Radiol* 23(12): 3393-404 (2013).
- [13] Sorbi S, Hert J, Erkinjuntti T, Fladby T, Gainotti G, Gurvit H, et al. EFNS-ENS Guidelines on the diagnosis and management of disorders associated with dementia. *Eur J Neurol* 19(9): 1159-79 (2012).
- [14] Frisoni GB, Bocchetta M, Chetelat G, Rabinovici GD, de Leon MJ, Kaye J, et al. Imaging markers for Alzheimer disease: which vs. how. *Neurology* 81(5): 487-500 (2013).
- [15] Jones DT, Machulda MM, Vemuri P, McDade EM, Zeng G, Senjem ML, et al. Age-related changes in the default mode network are more advanced in Alzheimer disease. *Neurology* 77(16): 1524-31 (2011).
- [16] Sheline YI, Raichle ME, Snyder AZ, Morris JC, Head D, Wang S, et al. Amyloid plaques disrupt resting state default mode network connectivity in cognitively normal elderly. *Biol Psychiatry* 67(6): 584-7 (2010).
- [17] Werner P, Barthel H, Drzezga A, Sabri O. Current status and future role of brain PET/MRI in clinical and research settings. *Eur J Nucl Med Mol Imaging* 42(3): 512-26 (2015).
- [18] Griffa A, Baumann PS, Thiran JP, Hagmann P. Structural connectomics in brain diseases. *Neuroimage* 80: 515-26 (2013).
- [19] Haller S, Nguyen D, Rodriguez C, Emch J, Gold G, Bartsch A, et al. Individual prediction of cognitive decline in mild cognitive impairment using support vector machine-based analysis of diffusion tensor imaging data. *J Alzheimers Dis* 22(1): 315-27 (2010).
- [20] Alsop DC, Dai W, Grossman M, Detre JA. Arterial spin labeling blood flow MRI: its role in the early characterization of Alzheimer's disease. *J Alzheimers Dis* 20(3): 871-80 (2010).
- [21] Binnewijzend MA, Kuijer JP, Benedictus MR, an der Flier WM, Wink AM, Wattjes MP, et al. Cerebral blood flow measured with 3D pseudocontinuous arterial spin-labeling MR imaging in Alzheimer disease and mild cognitive impairment: a marker for disease severity. *Radiology* 267(1): 221-30 (2013).
- [22] Xekardaki A, Rodriguez C, Montandon ML, Toma S, Tombeur E, Herrmann FR, et al. Arterial spin labeling may contribute to the prediction of cognitive deterioration in healthy elderly individuals. *Radiology* 274(2): 490-9 (2015).
- [23] Toledo JB, Arnold SE, Raible K, Brettschneider J, Xie SX, Grossman M, et al. Contribution of cerebrovascular disease in autopsy confirmed neurodegenerative disease cases in the National Alzheimer's Coordinating Centre. *Brain* 136(Pt 9): 2697-706 (2013).
- [24] Viswanathan A, Rocca WA, Tzourio C. Vascular risk factors and dementia: how to move forward? *Neurology* 72(4): 368-74 (2009).
- [25] Baskin A, Giannakopoulos P, Ratib O, Seimille Y, Assal F, Perani D, et al. PET radiotracers for molecular imaging in dementia. *Curr Radiopharm* 6(4): 215-30 (2013).
- [26] Albert MS, DeKosky ST, Dickson D, Dubois B, Feldman HH, Fox NC, et al. The diagnosis of mild cognitive impairment due to Alzheimer's disease: recommendations from the National Institute on Aging-Alzheimer's Association workgroups on diagnostic guidelines for Alzheimer's disease. *Alzheimers Dement* 7(3): 270-9 (2011).
- [27] McKhann GM, Knopman DS, Chertkow H, Hyman BT, Jack CR, Jr., Kawas CH, et al. The diagnosis of dementia due to Alzheimer's disease: recommendations from the National Institute on Aging-Alzheimer's Association workgroups on diagnostic guidelines for Alzheimer's disease. *Alzheimers Dement* 7(3): 263-9 (2011).
- [28] Sperling RA, Aisen PS, Beckett LA, Bennett DA, Craft S, Fagan AM, et al. Toward defining the preclinical stages of Alzheimer's disease: recommendations from the National Institute on Aging-Alzheimer's Association workgroups on diagnostic guidelines for Alzheimer's disease. *Alzheimers Dement* 7(3): 280-92 (2011).
- [29] Catana C, Drzezga A, Heiss WD, Rosen BR. PET/MRI for neurologic applications. *J Nucl Med* 53(12): 1916-25 (2012).
- [30] Cerami C, Della Rosa PA, Magnani G, Santangelo R, Marcone A, Cappa SF, et al. Brain metabolic maps in Mild Cognitive Impairment predict heterogeneity of progression to dementia. *Neuroimage Clin* 7187-94 (2015).
- [31] Drzezga A. Diagnosis of Alzheimer's disease with [18F]PET in mild and asymptomatic stages. *Behav Neurol* 21(1): 101-15 (2009).
- [32] Silverman DH, Small GW, Chang CY, Lu CS, Kung De Aburto MA, Chen W, et al. Positron emission tomography in evaluation of dementia: Regional brain metabolism and long-term outcome. *JAMA* 286(17): 2120-7 (2001).
- [33] Perani D, Della Rosa PA, Cerami C, Gallivanone F, Fallanca F, Vanoli EG, et al. Validation of an optimized SPM procedure for FDG-PET in dementia diagnosis in a clinical setting. *Neuroimage Clin* 6445-54 (2014).
- [34] Mosconi L, Tsui WH, Herholz K, Pupi A, Drzezga A, Lucignani G, et al. Multicenter standardized 18F-FDG PET diagnosis of mild cognitive impairment, Alzheimer's disease, and other dementias. *J Nucl Med* 49(3): 390-8 (2008).
- [35] Anchisi D, Borroni B, Franceschi M, Kerrouche N, Kalbe E, Beuthien-Beumann B, et al. Heterogeneity of brain glucose metabolism in mild cognitive impairment and clinical progression to Alzheimer disease. *Arch Neurol* 62(11): 1728-33 (2005).
- [36] Drzezga A, Grimmer T, Riemschneider M, Lautenschlager N, Siebner H, Alexopoulos P, et al. Prediction of individual clinical outcome in MCI by means of genetic assessment and (18)F-FDG PET. *J Nucl Med* 46(10): 1625-32 (2005).
- [37] Laforce R, Jr., Buteau JP, Paquet N, Verret L, Houde M, Bouchard RW. The value of PET in mild cognitive impairment, typical and atypical/unclear dementias: A retrospective memory clinic study. *Am J Alzheimers Dis Other Dement* 25(4): 324-32 (2010).
- [38] Nasrallah IM, Wolk DA. Multimodality imaging of Alzheimer disease and other neurodegenerative dementias. *J Nucl Med* 55(12): 2003-11 (2014).
- [39] Perani D. FDG-PET and amyloid-PET imaging: the diverging paths. *Curr Opin Neurol* 27(4): 405-13 (2014).
- [40] Clark CM, Schneider JA, Bedell BJ, Beach TG, Bilker WB, Mintun MA, et al. Use of florbetapir-PET for imaging beta-amyloid pathology. *JAMA* 305(3): 275-83 (2011).
- [41] Barthel H, Gertz HJ, Dresel S, Peters O, Bartenstein P, Buerger K, et al. Cerebral amyloid-beta PET with florbetaben (18F) in patients with Alzheimer's disease and healthy controls: a multicentre phase 2 diagnostic study. *Lancet Neurol* 10(5): 424-35 (2011).
- [42] Nordberg A, Carter SF, Rinne J, Drzezga A, Brooks DJ, Vandenberghe R, et al. A European multicentre PET study of fibrillar amyloid in Alzheimer's disease. *Eur J Nucl Med Mol Imaging* 40(1): 104-14 (2013).
- [43] Rowe CC, Villemagne VL. Brain amyloid imaging. *J Nucl Med* 52(11): 1733-40 (2011).
- [44] Fu L, Liu L, Zhang J, Xu B, Fan Y, Tian J. Comparison of dual-biomarker PIB-PET and dual-tracer PET in AD diagnosis. *Eur Radiol* 24(11): 2800-9 (2014).
- [45] Hsiao IT, Huang CC, Hsieh CJ, Hsu WC, Wey SP, Yen TC, et al. Correlation of early-phase 18F-florbetapir (AV-45/Amyvid) PET images to FDG images: preliminary studies. *Eur J Nucl Med Mol Imaging* 39(4): 613-20 (2012).
- [46] Wolk DA, Klunk W. Update on amyloid imaging: from healthy aging to Alzheimer's disease. *Curr Neurol Neurosci Rep* 9(5): 345-52 (2009).
- [47] Johnson KA, Minoshima S, Bohnen NI, Donohoe KJ, Foster NL, Herscovitch P, et al. Appropriate use criteria for amyloid PET: a report of the Amyloid Imaging Task Force, the Society of Nuclear Medicine and Molecular Imaging, and the Alzheimer's Association. *J Nucl Med* 54(3): 476-90 (2013).
- [48] Rowe CC, Ng S, Ackermann U, Gong SJ, Pike K, Savage G, et al. Imaging beta-amyloid burden in aging and dementia. *Neurology* 68(20): 1718-25 (2007).

- [49] Schlemmer HP, Pichler BJ, Schmand M, Burbar Z, Michel C, Ladebeck R, et al. Simultaneous MR/PET imaging of the human brain: feasibility study. *Radiology* 248(3): 1028-35 (2008).
- [50] Beyer T, Pichler B. A decade of combined imaging: from a PET attached to a CT to a PET inside an MR. *Eur J Nucl Med Mol Imaging* 36: 1S1-2 (2009).
- [51] Catana C, Wu Y, Judenhofer MS, Qi J, Pichler BJ, Cherry SR. Simultaneous acquisition of multislice PET and MR images: initial results with a MR-compatible PET scanner. *J Nucl Med* 47(12): 1968-76 (2006).
- [52] Judenhofer MS, Wehr HF, Newport DF, Catana C, Siegel SB, Becker M, et al. Simultaneous PET-MRI: a new approach for functional and morphological imaging. *Nat Med* 14(4): 459-65 (2008).
- [53] Zaidi H, Del Guerra A. An outlook on future design of hybrid PET/MRI systems. *Med Phys* 38(10): 5667-89 (2011).
- [54] Torigian DA, Zaidi H, Kwee TC, Saboury B, Udupa JK, Cho ZH, et al. PET/MR imaging: technical aspects and potential clinical applications. *Radiology* 267(1): 26-44 (2013).
- [55] Zaidi H, Ojha N, Morich M, Griesmer J, Hu Z, Maniawski P, et al. Design and performance evaluation of a whole-body Ingenuity TF PET-MRI system. *Phys Med Biol* 56(10): 3091-106 (2011).
- [56] Veit-Haibach P, Kuhn FP, Wiesinger F, Delso G, von Schultheiss G. PET-MR imaging using a tri-modality PET/CT-MR system with a dedicated shuttle in clinical routine. *MAGMA* 26(1): 25-35 (2013).
- [57] Disselhorst JA, Bezrukov I, Kolb A, Parl C, Pichler BJ. Principles of PET/MR Imaging. *J Nucl Med* 55(2): 2S-10S (2014).
- [58] von Schultheiss GK, Schlemmer HP. A look ahead: PET/MR versus PET/CT. *Eur J Nucl Med Mol Imaging* 36: 1S3-9 (2009).
- [59] Kolb A, Sauter AW, Eriksson L, Vandenbroucke A, Liu CC, Levin C, et al. Shine-Through in PET/MR Imaging: effects of the magnetic field on positron range and subsequent image artifacts. *J Nucl Med* 56(6): 951-4 (2015).
- [60] Cho ZH, Son YD, Kim HK, Kim ST, Lee SY, Chi JG, et al. Substructural hippocampal glucose metabolism observed on PET/MRI. *J Nucl Med* 51(10): 1545-8 (2010).
- [61] Jung JH, Choi Y, Jung J, Kim S, Lim HK, Im KC, et al. Development of PET/MRI with insertable PET for simultaneous PET and MR imaging of human brain. *Med Phys* 42(5): 2354 (2015).
- [62] Zaidi H, Montandon M-L, Alavi A. Advances in Attenuation Correction Techniques in PET. *PET Clin* 2(2): 191-217 (2007).
- [63] Wagenknecht G, Kaiser HJ, Mottaghy FM, Herzog H. MRI for attenuation correction in PET: methods and challenges. *MAGMA* 26(1): 99-113 (2013).
- [64] Hofmann M, Pichler B, Scholkopf B, Beyer T. Towards quantitative PET/MRI: a review of MR-based attenuation correction techniques. *Eur J Nucl Med Mol Imaging* 36 1S93-104 (2009).
- [65] Hofmann M, Steinke F, Scheel V, Charpiat G, Farquhar J, Aschoff P, et al. MRI-based attenuation correction for PET/MRI: a novel approach combining pattern recognition and atlas registration. *J Nucl Med* 49(11): 1875-83 (2008).
- [66] Kops ER, Herzog H. Template based Attenuation Correction for PET in MR-PET Scanners. *Nucl Sci Symp* 3786-3789 (2008).
- [67] Montandon ML, Zaidi H. Atlas-guided non-uniform attenuation correction in cerebral 3D PET imaging. *Neuroimage* 25(1): 278-86 (2005).
- [68] Rota Kops, E, H Herzog, Alternative Methods for Attenuation Correction for PET. *Images in MR-PET Scanners* 4327-4330 (2007).
- [69] Malone IB, Ansorge RE, Williams GB, Nestor PJ, Carpenter TA, Fryer TD. Attenuation correction methods suitable for brain imaging with a PET/MRI scanner: a comparison of tissue atlas and template attenuation map approaches. *J Nucl Med* 52(7): 1142-9 (2011).
- [70] Burgo N, Cardoso MJ, Thielemans K, Modat M, Pedemonte S, Dickson J, et al. Attenuation correction synthesis for hybrid PET-MR scanners: application to brain studies. *IEEE Trans Med Imaging* 33(12): 2332-41 (2014).
- [71] Schulz, V, Torres-Espallardo I, Renisch S, Hu Z, Ojha N, Bornert P, et al. Automatic, three-segment, MR-based attenuation correction for whole-body PET/MR data. *Eur J Nucl Med Mol Imaging* 38(1): 138-52 (2011).
- [72] Martinez-Moller, A, Souvatzoglou M, Delso G, Bundschuh RA, Chefd'hotel C, Ziegler SI, et al. Tissue classification as a potential approach for attenuation correction in whole-body PET/MRI: evaluation with PET/CT data. *J Nucl Med* 50(4): 520-6 (2009).
- [73] Andersen FL, Ladefoged CN, Beyer T, Keller SH, Hansen AE, Hojgaard L, et al. Combined PET/MR imaging in neurology: MR-based attenuation correction implies a strong spatial bias when ignoring bone. *Neuroimage* 84: 206-16 (2014).
- [74] Catana C, van der Kouwe A, Benner T, Michel CJ, Hamm M, Fenchel M, et al. Toward implementing an MRI-based PET attenuation-correction method for neurologic studies on the MR-PET brain prototype. *J Nucl Med* 51(9): 1431-8 (2010).
- [75] Zaidi H, Montandon ML, Slozman DO. Magnetic resonance imaging-guided attenuation and scatter corrections in three-dimensional brain positron emission tomography. *Med Phys* 30(5): 937-48 (2003).
- [76] Wagenknecht G, Rota Kops E, Kaffanke J, Tellmann L, Mottaghy F, Piroth M, et al., CT-based evaluation of segmented head regions for attenuation correction in MR-PET systems. *Knoxville, TN: IEEE* (2010); pp. 2793-2797.
- [77] Wagenknecht G, Rota Kops E, Tellmann L, Herzog H. Knowledge-based segmentation of attenuation-relevant regions of the head in T1-weighted MR images for attenuation correction in MR/PET systems. *Orlando, FL: IEEE* (2009); pp. 3338-3343.
- [78] Berker Y, Franke J, Salomon A, Palmowski M, Donker HC, Temur Y, et al. MRI-based attenuation correction for hybrid PET/MRI systems: a 4-class tissue segmentation technique using a combined ultrashort-echo-time/Dixon MRI sequence. *J Nucl Med* 53(5): 796-804 (2012).
- [79] KeeremanV, Fierens Y, Broux T, De Deene Y, Lonneux M, Vandenberghe S. MRI-based attenuation correction for PET/MRI using ultrashort echo time sequences. *J Nucl Med* 51(5): 812-8 (2010).
- [80] Boellaard R, Hofman MB, Hoekstra OS, Lammertsma AA. Accurate PET/MR quantification using time of flight MLAA image reconstruction. *Mol Imaging Biol* 16(4): 469-77 (2014).
- [81] Mehranian A, Zaidi H. Clinical assessment of emission- and segmentation-based MRI-guided attenuation correction in whole-body TOF PET/MRI. *J Nucl Med* 56(6): 877-883 (2015).
- [82] Rezaei A, Defrise M, Bal G, Michel C, Conti M, Watson C, et al. Simultaneous reconstruction of activity and attenuation in time-of-flight PET. *IEEE Trans Med Imaging* 31(12): 2224-33 (2012).
- [83] Tsoumpas C, Mackewn JE, Halsted P, King AP, Buerger C, Totman JJ, et al. Simultaneous PET-MR acquisition and MR-derived motion fields for correction of non-rigid motion in PET. *Ann Nucl Med* 24(10): 745-50 (2010).
- [84] Ouyang J, Li Q, El Fakhri G. Magnetic resonance-based motion correction for positron emission tomography imaging. *Semin Nucl Med* 43(1): 60-7 (2013).
- [85] Green MV, Seidel J, Stein SD, Tedder TE, Kempner KM, Kertzman C, et al. Head movement in normal subjects during simulated PET brain imaging with and without head restraint. *J Nucl Med* 35(9): 1538-46 (1994).
- [86] Piliput MN, Goble JC, Kassell NF. A noninvasive thermoplastic head immobilization system. Technical note. *J Neurosurg* 82(6): 1082-5 (1995).
- [87] Picard Y, Thompson CJ. Motion correction of PET images using multiple acquisition frames. *IEEE Trans Med Imaging* 16(2): 137-44 (1997).
- [88] Catana C, Benner T, van der Kouwe A, Byars L, Hamm M, Chonde DB, et al. MRI-assisted PET motion correction for neurologic studies in an integrated MR-PET scanner. *J Nucl Med* 52(1): 154-61 (2011).
- [89] Chun SY, Reese TG, Ouyang J, Guerin B, Catana C, Zhu X, et al. MRI-based nonrigid motion correction in simultaneous PET/MRI. *J Nucl Med* 53(8): 1284-91 (2012).
- [90] Ullisch MG, Scheins JJ, Weirich C, Rota Kops E, Celik A, Tellmann L, et al. MR-based PET motion correction procedure for simultaneous MR-PET neuroimaging of human brain. *PLoS One* 7(11): e48149 (2012).
- [91] Haller S, Monsch AU, Richiardi J, Barkhof F, Kressig RW, Radue EW. Head motion parameters in fMRI differ between patients with mild cognitive impairment and Alzheimer disease versus elderly control subjects. *Brain Topogr* 27(6): 801-7 (2014).
- [92] Zaidi H, Montandon M-L, Assal F. Structure-function-based quantitative brain image analysis. *PET Clin* 5(2): 155-168 (2010).

- [93] Garibotto V, Forster S, Haller S, Vargas MI, Drzezga A. Molecular Neuroimaging with PET/MRI. *Clin Trans Imag* 1(1): 53-63 (2013).
- [94] Ishii K, Willoch F, Minoshima S, Drzezga A, Ficaro EP, Cross DJ, et al. Statistical brain mapping of 18F-FDG PET in Alzheimer's disease: validation of anatomic standardization for atrophied brains. *J Nucl Med* 42(4): 548-57 (2001).
- [95] Nishimiya M, Matsuda H, Imabayashi E, Kuji I, Sato N. Comparison of SPM and NEUROSTAT in voxelwise statistical analysis of brain SPECT and MRI at the early stage of Alzheimer's disease. *Ann Nucl Med* 22(10): 921-7 (2008).
- [96] Roland PE, Graufelds CJ, WH J, Ingelman L, Andersson M, Ledberg A, et al. Human brain atlas: For high-resolution functional and anatomical mapping. *Hum Brain Mapp* 1(3): 173-84 (1994).
- [97] Friston KJ, Holmes AP, Worsley KJ, Poline J-P, Frith CD, Frackowiak RSJ. Statistical parametric maps in functional imaging: A general linear approach. *Hum Brain Mapp* 2(4): 189-210 (1995).
- [98] Della Rosa PA, Cerami C, Gallivanone F, Prestia A, Caroli A, Castiglioni I, et al. A standardized [18F]-FDG-PET template for spatial normalization in statistical parametric mapping of dementia. *Neuroinformatics* 12(4): 575-93 (2014).
- [99] Pagani M, Salmaso D, Borbely K. Optimisation of statistical methodologies for a better diagnosis of neurological and psychiatric disorders by means of SPECT. *Nucl Med Rev Cent East Eur* 8(2): 140-9 (2005).
- [100] Minoshima S, Berger KL, Lee KS, Mintun MA. An automated method for rotational correction and centering of three-dimensional functional brain images. *J Nucl Med* 33(8): 1579-85 (1992).
- [101] Van Laere KJ, Warwick J, Versijpt J, Goethals I, Audenaert K, Van Heerden B, et al. Analysis of clinical brain SPECT data based on anatomic standardization and reference to normal data: an ROC-based comparison of visual, semiquantitative, and voxel-based methods. *J Nucl Med* 43(4): 458-69 (2002).
- [102] Herholz K, Salmon E, Perani D, Baron JC, Holthoff V, Frolich L, et al. Discrimination between Alzheimer dementia and controls by automated analysis of multicenter FDG PET. *Neuroimage* 17(1): 302-16 (2002).
- [103] Haense C, Herholz K, Jagust WJ, Heiss WD. Performance of FDG PET for detection of Alzheimer's disease in two independent multicentre samples (NEST-DD and ADNI). *Dement Geriatr Cogn Disord* 28(3): 259-66 (2009).
- [104] Hosaka K, Ishii K, Sakamoto S, Sadato N, Fukuda H, Kato T, et al. Validation of anatomical standardization of FDG PET images of normal brain: comparison of SPM and NEUROSTAT. *Eur J Nucl Med Mol Imaging* 32(1): 92-7 (2005).
- [105] von Borczyskowski D, Wilke F, Martin B, Brenner W, Clausen M, Mester J, et al. Evaluation of a new expert system for fully automated detection of the Alzheimer's dementia pattern in FDG PET. *Nucl Med Commun* 27(9): 739-43 (2006).
- [106] Garibotto V, Heinzer S, Vulliemoz S, Guignard R, Wissmeyer M, Seeck M, et al. Clinical applications of hybrid PET/MRI in neuroimaging. *Clin Nucl Med* 38(1): e13-8 (2013).
- [107] Schwenzer NF, Stegger L, Bisdas S, Schraml C, Kolb A, Boss A, et al. Simultaneous PET/MR imaging in a human brain PET/MR system in 50 patients--current state of image quality. *Eur J Radiol* 81(11): 3472-8 (2012).
- [108] Jena A, Taneja S, Goel R, Renjen P, Negi P. Reliability of semiquantitative (1)(8)F-FDG PET parameters derived from simultaneous brain PET/MRI: a feasibility study. *Eur J Radiol* 83(7): 1269-74 (2014).
- [109] Moodley KK, Perani D, Minati L, Della Rosa PA, Pennycook F, Dickson JC, et al. Simultaneous PET-MRI studies of the concordance of atrophy and hypometabolism in syndromic variants of Alzheimer's disease and frontotemporal dementia: an extended case series. *J Alzheimer's Dis* 46(3): (2015).
- [110] Drzezga A, Barthel H, Minoshima S, Sabri O. Potential clinical applications of PET/MR imaging in neurodegenerative diseases. *J Nucl Med* 55(2): 47S-55S (2014).
- [111] Barthel H, Schroeter ML, Hoffmann KT, O Sabri. PET/MR in dementia and other neurodegenerative diseases. *Semin Nucl Med* 45(3): 224-33 (2015).
- [112] Zhang K, Herzog H, Mauler J, Filss C, Okell TW, Kops ER, et al. Comparison of cerebral blood flow acquired by simultaneous [15O]water positron emission tomography and arterial spin labeling magnetic resonance imaging. *J Cereb Blood Flow Metab* 34(8): 1373-80 (2014).
- [113] Aiello M, Salvatore E, Cachia A, Pappata S, Cavalieri C, Prinster A, et al. Relationship between simultaneously acquired resting-state regional cerebral glucose metabolism and functional MRI: A PET/MR hybrid scanner study. *Neuroimage* 113111-21 (2015).
- [114] Andersen JB, Henning WS, Lindberg U, Ladefoged CN, Hojgaard L, Greisen G, et al. Positron emission tomography/magnetic resonance hybrid scanner imaging of cerebral blood flow using O-water positron emission tomography and arterial spin labeling magnetic resonance imaging in newborn piglets. *J Cereb Blood Flow Metab* 35(11): 1703-10 (2015).
- [115] Vitali P, Maccagnano E, Caverzasi E, Henry RG, Haman A, Torres-Chae C, et al. Diffusion-weighted MRI hyperintensity patterns differentiate CJD from other rapid dementias. *Neurology* 76(20): 1711-9 (2011).
- [116] Kantarci K, Petersen RC, Boeve BF, Knopman DS, Weigand SD, O'Brien PC, et al. DWI predicts future progression to Alzheimer disease in amnestic mild cognitive impairment. *Neurology* 64(5): 902-4 (2005).
- [117] Ray KM, Wang H, Chu Y, Chen YF, Bert A, Hasso AN, et al. Mild cognitive impairment: apparent diffusion coefficient in regional gray matter and white matter structures. *Radiology* 241(1): 197-205 (2006).
- [118] Graff-Radford J, Kantarci K. Magnetic resonance spectroscopy in Alzheimer's disease. *Neuropsychiatr Dis Treat* 9687-96 (2013).
- [119] Villemagne VL, Fodero-Tavoletti MT, Masters CL, Rowe CC. Tau imaging: early progress and future directions. *Lancet Neurol* 14(1): 114-24 (2015).
- [120] Wehner J, Weissler B, Dueppenbecker P, Gebhardt P, Schug D, Ruettner W, et al. PET/MRI insert using digital SiPMs: Investigation of MR-compatibility. *Nucl Instrum Methods Phys Res A* 734116-121 (2014).
- [121] Olcott P, Kim E, Hong K, Lee BJ, Grant AM, Chang CM, et al. Prototype positron emission tomography insert with electro-optical signal transmission for simultaneous operation with MRI. *Phys Med Biol* 60(9): 3459-78 (2015).